

SEMI-ANNUAL REPORT

TITLE OF GRANT:

Electronic Characterization of Defects in Narrow Gap Semiconductors

TYPE OF REPORT:

Brief Summary of Project

NAME OF PRINCIPAL INVESTIGATOR:

James D. Patterson

PERIOD COVERED BY THE REPORT:

November 25, 1992 to June 25, 1993

(MID YEAR REPORT)

NAME AND ADDRESS OF GRANTEE INSTITUTION:

Florida Institute of Technology
150 West University Boulevard
Melbourne, FL 32901

GRANT NUMBER:

NAG8-941

George C. Marshall Space Flight Center
Marshall Space Flight Center, AL 35812
(Technical Officer: Sandor L. Lehoczky, ES75)

(NASA-CR-193563) ELECTRONIC
CHARACTERIZATION OF DEFECTS IN
NARROW GAP SEMICONDUCTORS
Semiannual Report, 25 Nov. 1992 -
25 Jun. 1993 (Florida Inst. of
Tech.) 59 p

N94-10819

Unclas

G3/76 0179485

PERSONNEL

Dr. James D. Patterson, Principal Investigator
Professor and Head
Physics and Space Sciences Department
Florida Institute of Technology

A handwritten signature in cursive script that reads "James D. Patterson".

Dr. Weigang Li, Post-Doctoral Research Associate
Physics and Space Sciences Department
Florida Institute of Technology

A handwritten signature in cursive script that reads "Weigang Li".

ELECTRONIC CHARACTERIZATION OF DEFECTS IN NARROW GAP SEMICONDUCTORS

- I. Introduction
- II. Deep Levels of Point Defects in Semiconductors
 - A. Green's Function Method
 - B. Comments in Ideal Vacancy Model
 - C. Band Structure of II-VI Semiconductors
 - D. Lattice Relaxation and Molecule Dynamics Approach
 - E. Interstitial Defects - Brief Comments
 - F. Summary of Results for MCT, MZT and MZS for Substitutional Defects
- III. Shallow Levels in II-VI Materials
 - A. General Discussion
 - B. Other Complications
- IV. Appendices
 - A. Some Basic References
 - B. Green Function
 - 1. Summary of Some Standard Results
 - 2. Analytical Results
 - 3. Determination of $G^{\circ}(E)$ - Vogl Band Structure
 - 4. Determination of V - Hjalmarson's Deep Level Theory
 - C. Details of Shallow Impurity Levels

TABLES

Table I: Types of Point Defects

Table II: Materials

Table III: Brief Properties of Shallow and Deep Levels in II-VI Compounds

Table IV: Summary of Calculations which we have done on Deep Levels

Table V: Bond Lengths, parameters α_s and α_p , and p-like deep levels

FIGURES

Figure 1: Deep Levels in MZT

Figure 2: Deep Levels in MZS

Figure 3: Effects of Lattice Relaxation in MZT

Figure 4: Effects of Lattice Relaxation in MCT

Figure 5: Effects of Lattice Relaxation in MZS

Figure 6: Vacancy Levels in MZT

I. INTRODUCTION^(1,2)

The study of point defects in semiconductors has a long and honorable history (see Table I). In particular, the detailed understanding of shallow defects in common semiconductors traces back to the classic work of Kohn and Luttinger. However, the study of defects in narrow gap semiconductors represents a much less clear story. Here, both shallow defects (caused by long range potentials) and deep defects (from short range potentials) are far from being completely understood.

The study of narrow gap semiconductors (see Table II) is important to NASA because typical ones such as Mercury Cadmium Telluride and Mercury Zinc Telluride are difficult to grow uniformly under the stress of gravity induced convection. Also, the narrow gap semiconductors are useful for infrared detection which in turn is useful for remote sensing and a variety of military purposes.

One aspect of studying crystal perfection is to study the natural and artificial defects which appear in these materials. In our study we calculate the properties of numerous examples of deep defects and discuss some problems associated with the study of shallow defects (see Table III). All defects we study are point defects. Until one can identify and characterize defects, it is impossible to make clear statements about crystal perfection.

A full characterization of crystal perfection involves not only a theoretical study of all common defects but also experimental verification of the models. The simplest model of shallow defects assumes they are fully ionized. There is not a lot one can do with such a model. However, refinements tend to get one into many complications, as we discuss in the appendix. Donor defects can perhaps be best studied by photoluminescence experiments. It is also of interest that the scanning tunneling microscope, which can be used to measure the local density of states, can also be used to study deep defect energy levels.

In this study, all results are calculational and our focus is on the chemical trends of deep levels in narrow gap semiconductors (see Table IV). We study substitutional (including antisite), interstitial and ideal vacancy defects. For substitutional and interstitial impurities, the effects of relaxation are included. For materials like $\text{Hg}_{1-x}\text{Cd}_x\text{Te}$, we study how the deep levels vary with x , of particular interest is what substitutional and interstitial atoms yield energy levels in the gap i.e. actually produce deep ionized levels (see Table IV). Also, since the main technique utilized is Green's functions, we include some summary of that method.

II. DEEP LEVELS OF POINT DEFECTS IN SEMICONDUCTORS

A. Green's Function Method⁽³⁻⁶⁾

Let us suppose that an atom of the perfect crystal is replaced by a defect. If the Hamiltonian of the perfect crystal is H_0 and if the change in potential produced by the defect is V , then Schrodinger's equation becomes

$$(H_0 + V)|\Psi\rangle = E|\Psi\rangle. \quad (1)$$

The host crystal's Green's function is defined as

$$G^0(E) = (E - H_0)^{-1}. \quad (2)$$

Combining these two equations, we have

$$(I - G^0(E)V)|\Psi\rangle = 0. \quad (3)$$

The defect energy levels E in the band gap of a semiconductor are thus given by non-trivial solutions of the determinantal equation:

$$\text{Det}(I - G^0(E)V) = 0. \quad (4)$$

For a point defect in a tetrahedral site of a zinc blende material, the point group is T_d . Such a defect can have both non-degenerate A_1 (s - like) state or triply degenerate T_2 (p - like) states. Assuming these states, Eqn (4) can be factored as

$$\det[I - G^0(E)V] = \prod_{i=0}^3 \det[I_i - G_i^0 V_i] = 0 \quad (5)$$

for $i = 0$ corresponding to A_1 states and $i = 1, 2, 3$ to T_2 states.

For A_1 states only

$$\det[I_s - G_s^0 V_s] = 0 \quad (6)$$

and for the T_2 states

$$\det \left[I_p - G_p^0 V_p \right] = 0, \quad (7)$$

for suitably defined G_s^0, V_s and G_p^0, V_p .

Using the equations $U_s = 1/G_{aa}^s$ and $U_p = 1/G_{aa}^p$ (see Appendix B4), the deep levels in the band gap can be determined as a function of U_s and U_p , which is what we mean by impurity potential in Figs. 3 - 6. Here $U_s = \beta_s (E_{\text{imp}}^s - E_{\text{host}}^s)$ and $U_p = \beta_p (E_{\text{imp}}^p - E_{\text{host}}^p)$, where E_{imp} and E_{host} are the ground state orbital energies of defect and host atom, respectively. The relationship between U_s, U_p and V is explained in the appendix. Since the Green's function $G^0(E)$ is a function of energy E , we can calculate $G^0(E)$ for E in the band gap. Thus we can obtain a plot of U_s vs E or E vs U_s (and similarly for U_p). For each substitutional defect, the difference in energies will be determined as will $\beta_s, (\beta_p)$. Thus we can locate the deep defect energy levels.

B. Comments on Ideal Vacancy Model⁽⁷⁾

Vacancies are the most common native defects. The ideal vacancy model is an often used model for predicting deep vacancy levels. This model is described in detail in the paper by Das Sarma and Madhukar. The model assumes that a vacancy is formed by removing an atom from the crystal, but leaving all other atoms in the same position. Das Sarma and Madhukar proved that this is equivalent to setting U_s and U_p equal to infinity. From our previous equations, this is equivalent to setting

$$\begin{aligned} G_{aa}^s(E) &= 0 \\ G_{aa}^p(E) &= 0 \end{aligned} \tag{8}$$

This, in turn, is equivalent to setting atomic orbital energies equal to ∞ .

C. Band Structure Theory of II-VI Semiconductors⁽⁸⁾

Unlike III-V semiconductors, II-VI semiconductors may have strong spin-orbital coupling, which must be included in the band structure calculations. Based on Vogl et al. band structure theory, Kobayashi proposed a theory for II-VI semiconductors which included spin-orbital coupling. The Hamiltonian for the perfect crystal in this theory is (assume that the defect is on the anion site)

$$H_o = \sum \left(|i a \sigma \vec{o}\rangle E_i^a \langle i a \sigma \vec{o}| + |i c \sigma \vec{d}\rangle E_i^c \langle i c \sigma \vec{d}| \right) + \sum \left[|i a \sigma \vec{o}\rangle V_{ij} \langle j c \sigma \vec{d}| + \text{h.c.} \right] + H_{so}, \quad (9)$$

where σ is the spin, \vec{o} specifies the unit cell, and \vec{d} is the nearest-neighbor vector. H_{so} is the spin-orbit Hamiltonian, which can be written

$$H_{so} = \sum \left[|i a \sigma \vec{o}\rangle 2\lambda_a \vec{L}_a \cdot \vec{\sigma}_a \langle j a \sigma \vec{o}| + |i c \sigma \vec{d}\rangle 2\lambda_c \vec{L}_c \cdot \vec{\sigma}_c \langle j c \sigma \vec{d}| \right], \quad (10)$$

where λ_a and λ_c are the spin-orbit parameters. As usual, the band structures of the alloys were obtained within the virtual crystal approximation.

However, for most point defects that we are interested in, the spin-orbit interaction is weak and can be ignored. Then, including the degeneracy due to spin just doubles the degeneracy of each level. This makes the A_1 states doubly degenerate, and the T_2 states six fold degenerate. For this case, the previous Hjalmarson et al theory is still valid.

D. Lattice Relaxation and Molecular Dynamics Approach⁽⁹⁻¹³⁾

1. When the off-diagonal elements of the defect potential are equal to zero, the effects of the lattice relaxation are excluded since only these elements are related to defect-bond length. To include these effects, we must include the off-diagonal elements of the defect potential. Using the nearest-neighbor approximation, the form of the defect potential is

$$V = \sum V_i = \sum_i |i a \vec{o} \rangle V_i \langle i a \vec{o} | + \sum_{i,j} |i a \vec{o} \rangle \alpha_{ij} \langle j c \vec{d} | \quad (11)$$

where i can be s or p , and α_{ij} define the off diagonal elements. When all the symmetries are built in, we find the form of the matrix element V_i is

$$V_i = \begin{matrix} U_{aa}^i & \alpha & \alpha & \alpha & \alpha \\ & \alpha & & & \\ \alpha & & & 0 & \\ & \alpha & & & \\ & & \alpha & & \\ & & & \alpha & \end{matrix} \quad (12)$$

The determinantal equation then leads to the following:

$$U_i = \frac{1}{G_{aa}^i} - \frac{G_{ca}^i + G_{ac}^i}{G_{aa}^i} 4 \alpha_i + \frac{4G_{ca}^i G_{ac}^i - G_{cc}^i G_{aa}^i - 3G_{aa}^i G_{cc}^i}{G_{aa}^i} 4 \alpha_i^2, \quad (13)$$

where G_{cc}^i is the elements of Green's function matrix coupling two nearest-neighbor host atoms. This gives an implicit equation for the i - symmetric deep levels E as a function of U_i and α_i .

The form of α can be inferred from arguments due to Harrison which imply that the nearest neighbor matrix elements scale as the inverse bond length squared. We thus find

$$\alpha_i = -c_i \left(\frac{1}{d_I^2} - \frac{1}{d_H^2} \right) \quad (14)$$

where d_I is the bond length between the defect and one of the nearest neighbors, and d_H is the bond length of the host crystal, with C_i being a proportionality constant. Since α_i is related to d_I it is also directly related to the lattice relaxation. Further the sign of α_i determines the direction of lattice relaxation.

If we can determine α for a particular defect, the deep levels induced by this defect can then be predicted by the previous equation. In order to determine α , we need to calculate d_I and d_H . For well known semiconductors d_H is known. The determination of d_I is more difficult, and we now discuss this.

2. Molecular Dynamics Approach

- (a) In order to calculate α for a particular defect in a host, the defect bond length must be specified. A simple model will first be presented, and then the more general molecular dynamics approach. The simple model uses the concept of covalent radius. It is assumed that

$$d_I = r_I + r_H \quad (15)$$

where r_I and r_H are the covalent radii of the defect and the nearest-neighbor atoms respectively. Such radii are tabulated for most atoms of interest in the present study. The host bond length is given by

$$d_H = r_H^a + r_H^c \quad (16)$$

For a particular defect in a host, if $d_I > d_H$ we have outward relaxation. If $d_I < d_H$, we have inward relaxation.

This simple model works very well for most group IV and III-V semiconductors. However, it is not suitable for II-VI semiconductors because they are not purely covalent materials, but a mixture of covalent and ionic bonds. For these we must use a molecular dynamics approach.

- (b) For an ideal defect, the four nearest-neighbor host atoms will remain in their perfect-crystal positions. However, in a more realistic

treatment, these atoms experience a net force and the lattice distorts to a new configuration where that force is zero. The total force on one of the nearest-neighbor atoms can be divided into repulsive and attractive parts, which can be represented as

$$F_x = F_x^r + F_x^a \quad (17)$$

where x is along the defect-host bond direction. The origin of F_x^r is the repulsion between electrons in overlapping states, and this force can be computed from the empirical relation

$$F_x^r = A/d_I^5 \quad (18)$$

where A is a constant determined by the condition

$$F_x^r(d_H) = F_x^a(d_H) \quad (19)$$

which assumes the same functional form for $\frac{\partial V}{\partial x}$ for the host crystal as for the host crystal with defect. The attractive force F_x^a can be computed by use of the equation

$$F_x^a = \frac{1}{\pi} \text{Im Tr} \left[\int_{-\infty}^{\epsilon_F} \epsilon G \frac{\partial V}{\partial x} G d\epsilon \right] \quad (20)$$

where ϵ_F is the Fermi energy, G is the Green's function matrix including the defect and V is the defect potential (see Eqn. B38).

Using these two equations and beginning with the nearest neighbor host atoms in their perfect-crystal positions, we can calculate the motion of each of these atoms for a small time interval, Δt , using Newton's second law with the standard molecular dynamics approach. One lets the process continue until the net force approaches zero. Thus d_I is determined.

E. Interstitial Defects - Brief Comments (14-15)

Self interstitial impurities and vacancies are the most important native defects in semiconductors. In II-VI materials, it is believed that a substitutional group - I acceptor may spontaneously move to an interstitial site.

For a substitutional defect in zinc blende structure semiconductors, the defect has a tetrahedral symmetry in the materials. That is, there are four nearest-neighbor atoms and twelve second-nearest-neighbor atoms around the defect. If the distance between the defect and the nearest neighbor is d , then the distance between the defect and its second neighbor is $1.64 d$. The situation of tetrahedral-site interstitial impurities is different. In this case, there are four nearest neighbors around an interstitial impurity with distance d' , but only six second neighbors around it with a slightly greater distance $1.15 d'$. Hence, the nearest-neighbor approximation, which is often used for substitutional defects, is not acceptable for interstitial impurities.

We will calculate results for deep levels introduced by interstitial impurities in MCT, MZT, and MZS. The theory we will use will take into account the above complications but will be somewhat similar to what we have done before. We will give our results in the final report.

F. Summary of Results for MCT, MZT and MZS for Substitutional Defect

In Table 4, we summarize the results of several calculations we have done including both substitutional vacancy and antisite defects. In the final report, we will include these, as well as results in interstitial defects. Here we just give some typical results. In Table 5 we give a few typical examples of the calculations including the effects of lattice relaxation.

In Figure 1 (for MZT), we show several possible cation-site s-like (A_1) levels which may be formed by (for example) Te (Antisite), C, At and I as a function of composition x . The vacancy level below the valence band edge is considered because it is possible that lattice relaxation or other effects may raise it into the bandgap. In Figure 2 (For MZS), we see anion site, p-like (T_2) levels due to Cd, Zn (antisite), Mg and Be as function of composition x .

In Figs. 3, 4, 5 we summarize some results including the effects of lattice relaxation for anion-site p-like deep levels which we can get for MZT ($x = 0.15$), MCT ($x = 0.22$) and MZS ($x = .08$). In each case the top of the valence band is at $E = 0.0$ and the bottom of the conduction band is at $E = 0.1$. In Fig. 3, we see that Zn may have an impurity level in the band gap for $\alpha = 0$ (no relaxation). Similar comments may be made about Cd in MCT and Be in MZS. In each of these particular cases relaxation may take the level out of the band gap or deeper in the band gap (see Table 5). In Fig. 6, the ideal vacancy levels are modeled by setting the impurity energy = $\pm \infty$ (or - 120 is nearly the same). We see the vacancy levels appear below the top of the valence band for this case. For other situations we do find some vacancy levels in the band gap for MZS. We will provide a detailed summary of our results in the final report.

III. SHALLOW IMPURITY LEVELS IN II-VI MATERIALS

A. General Discussion⁽¹⁶⁻¹⁷⁾

We give , in the appendix, a fairly complete description of shallow defects in narrow gap semiconductors which can be modeled by the Kane Model⁽¹⁸⁾. Much of this materials comes from the book by Bastard⁽¹⁹⁾. The essential fact to note is that band mixing causes the situation to be much more complication than a hydrogenic model - except in the crudest approximate. In any case, for shallow impurity levels, we always assume a long range potential with perhaps a central cell connection if some refinements are necessary.

The main purpose of including Appendix C is to give one a feel for the complexity of the problem and to show why, since the binding energy can never be appreciable, that one often assumes total ionization of the shallow levels.

B. Other Complexities^(20, 21)

We have already mentioned that the donor ionization energy may be so small that it is only sensible to assume its total ionization.

In addition with a large density of states, the donor levels may split into a band which may merge with the conduction band. The merging of the donor levels with the conduction band seems to be a common occurrence for Mercury Cadmium Telluride with $x < 0.2$. There are other reasons for the merging of the donor levels with the conduction band. Donor levels can be screened by the electrons in the conduction band, and this screening can decrease the binding energy (Neumark). In addition, when the binding energy gets small enough, the donor wavefunctions may hybridize with the band functions and again we get merging (Lowney).

TABLE 1
Types of Point Defects

Substitutional Atoms

Interstitial Atoms (Self or Foreign)

Vacancy

Antisite Defect in Compound Semiconductor

TABLE 2

Materials

MCT	HgCdTe	$\text{Hg}_{1-x}\text{Cd}_x\text{Te}$
MZT	HgZnTe	$\text{Hg}_{1-x}\text{Zn}_x\text{Te}$
MZS	HgZnSe	$\text{Hg}_{1-x}\text{Zn}_x\text{Se}$

TABLE 3**Brief Properties of Shallow and Deep Levels in II-VI Compounds**

	<u>DEEP LEVEL</u>	<u>SHALLOW LEVEL</u>
Definition	Originates from short range potential	Originates from long range potential
Wave Functions	Typically mix with Valance and Conduction band	May mix only with adjacent band to level
Energies	Often have ionization energies comparable to half of gap energy - not a Hydrogen like spectrum - use tight binding approximation	Usually have ionization energies much less than gap energy - have a Hydrogen like spectrum as modified by dielectric constant effective mass, or other complications
Properties	Act as recombination centers, compensators, and facilitators for electron-hole generation	These supply carriers and hence control conductivity
Complications	Hard to identify appropriate models Non parabolic bands	Questions of screening (which may be site dependent) and merging with band Non parabolic bands and band mixing Polar nature of lattice, degeneracy or near degeneracy of bands can also cause complications
Examples	Vacancy, substitutional atom, antisite, interstitial atom	Hg vacancy, In on metal site plus many others as predicted by periodic table
Historical Theory	Slater-Koster	Kohn-Luttinger Effective Mass

TABLE 4

Summary of Calculations which we Have Done on Deep Levels

No Relaxation

MZT

cation-site-s-like - Te (antisite), C, At, I
 cation-site-p-like F
 anion-site-p-like Cd, Hg (antisite), Zn (antisite), Mg vs. x
 anion-site-s-like there are no deep levels predicted in the band gap
 several $x = 0.3$ levels - both s- and p-like
 several $x = 0.2$ levels - p-like
 cation-site-s-like vacancy level is below the valance band edge about 0.4 eV

MZS

anion site p-like Cd, Zn (antisite), Mg, Be
 cation site p-like Vacancy vs. x
 cation site s-like Vacancy
 anion-site s-like there are no deep levels predicted in the band gap

With Relaxation (when the parameter $\alpha = 0$, the use of no relaxation is included).

MZT

anion-site	p-like	$x = 0.15$	
cation-site	s- and p-like	$x = 0.15$	
anion-site	p-like	$x = 0.3$	$\alpha = -0.4, -0.2, 0.0, 0.2, 0.4$
cation-site	s- and p-like	$x = 0.3$	
Vacancy	s- and p-like	$x = 0.15$	

MCT

anion-site	p-like	$x = 0.22$	$\alpha = -0.4, -0.2, 0.0, 0.2, 0.4$
cation-site	s- and p-like	$x = 0.22$	

MZS

anion-site	s- and p-like	$x = 0.08$	$(\alpha = -0.4, -0.2, 0.0, 0.2, 0.4)$
------------	---------------	------------	--

TABLE 5**Bond Lengths****parameter α_s α_p and p-like deep levels with or without relaxation**

System	d_H (Å)	d_I (Å)	α_s (eV)	α_p (eV)	deep levels (no relax)	deep levels (relaxed)
MZT:HgTe	2.74	2.80	0.07	- 0.04	C. B. ^a	C. B.
MZT:ZnTe	2.74	2.58	- 0.22	0.13	0.9 Eg ^b	0.4 Eg
MCT:CdTe	2.54	2.71	0.20	- 0.11	0.98 Eg	C. B.

a. C. B. means conduction band resonance.

b. Eg means the energy band gap.

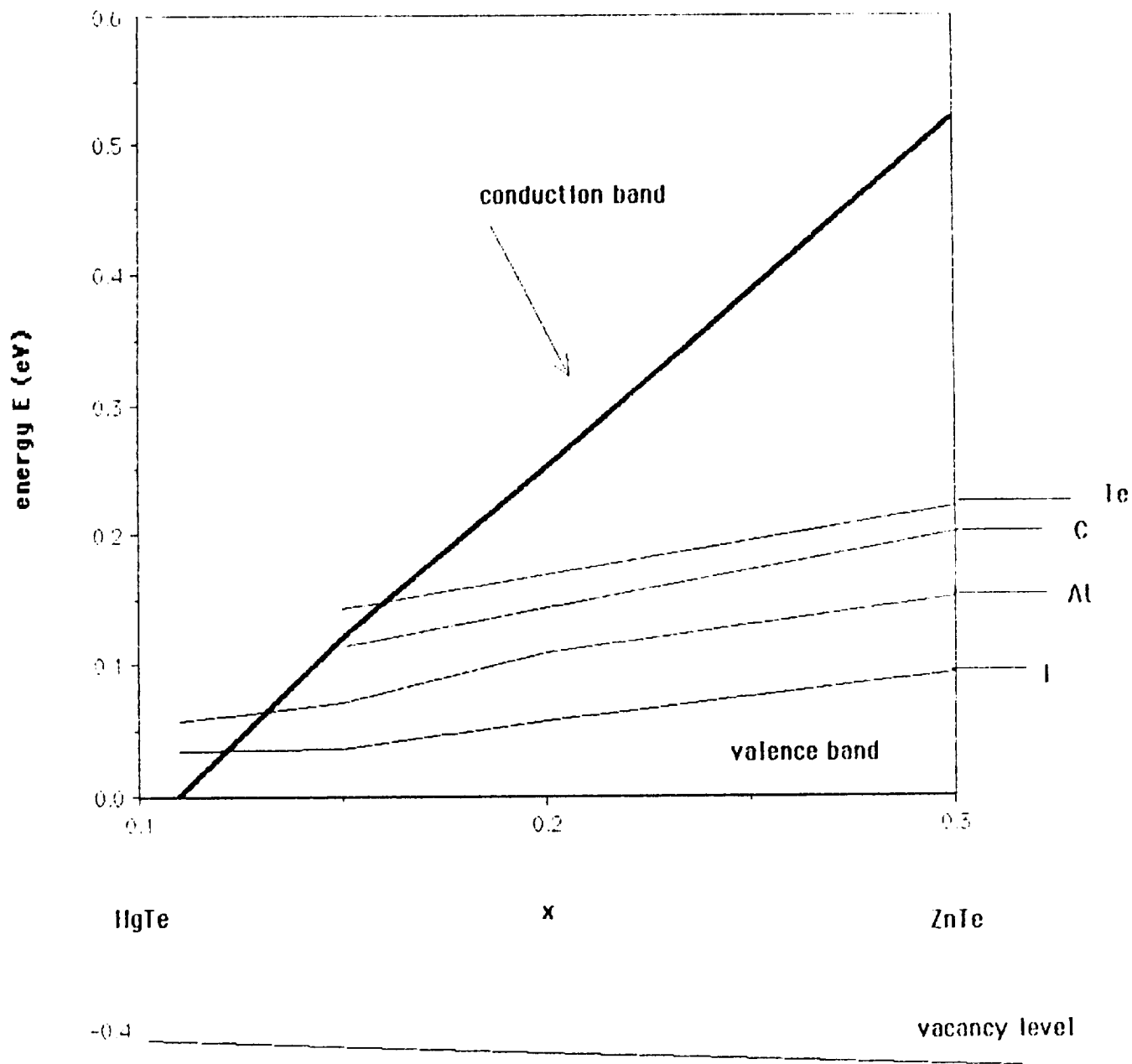


FIGURE 1

Deep Levels in MZT (cation site, s-like)

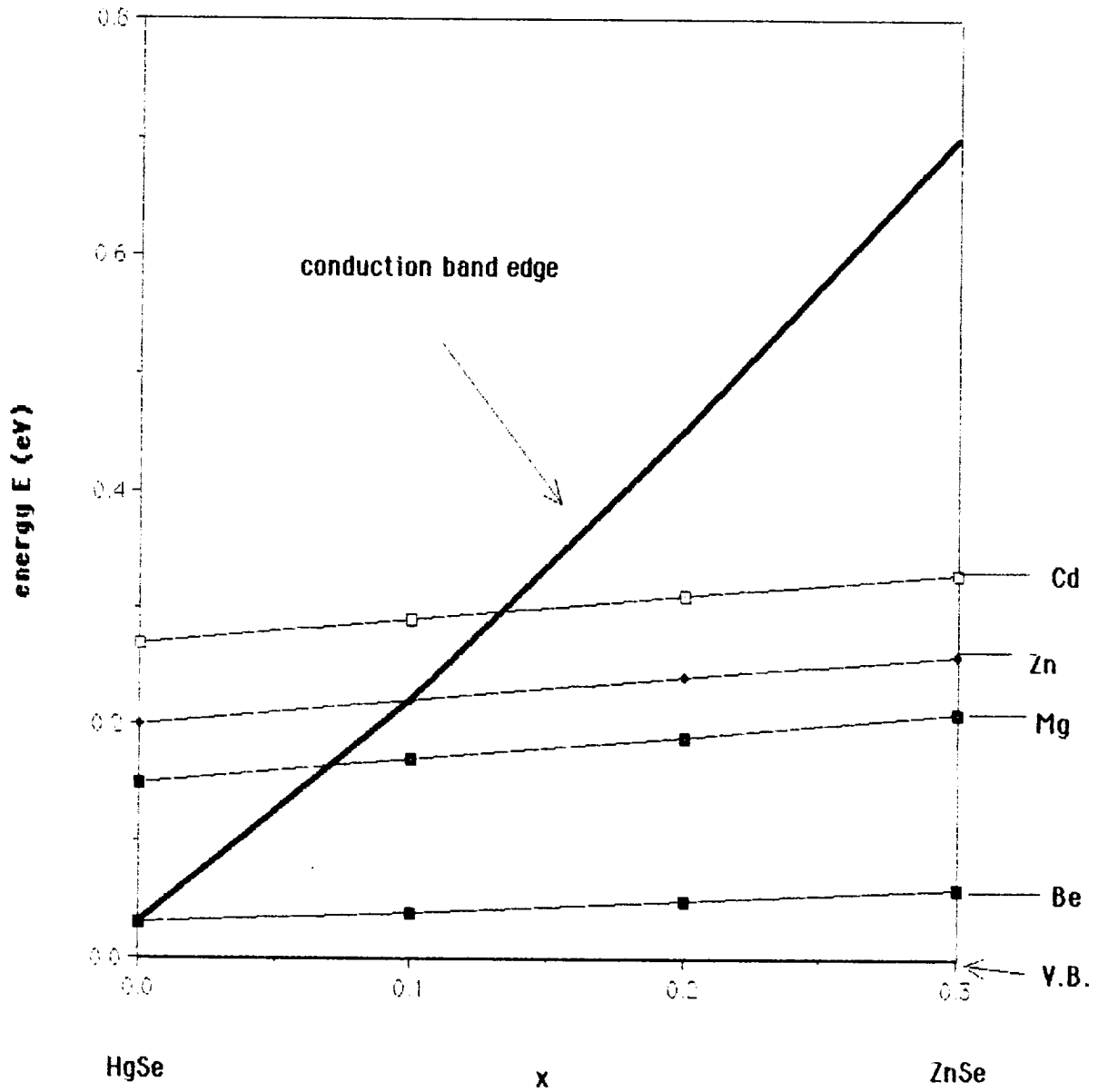


FIGURE 2

Deep Levels in MZS (anion site, p-like)

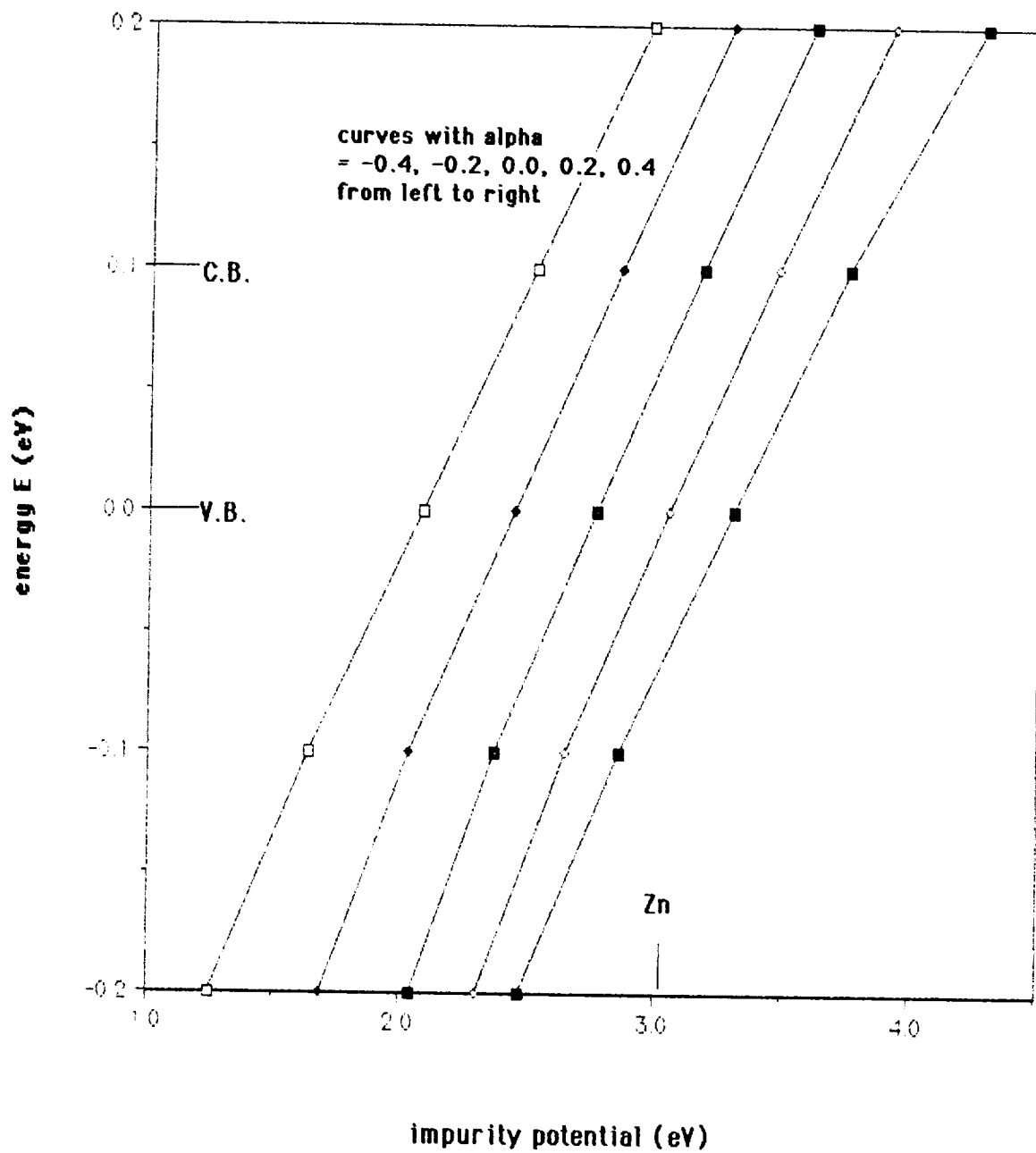


FIGURE 3

Effects of Lattice Relaxation on Deep Levels in MZT (anion site, p-like)

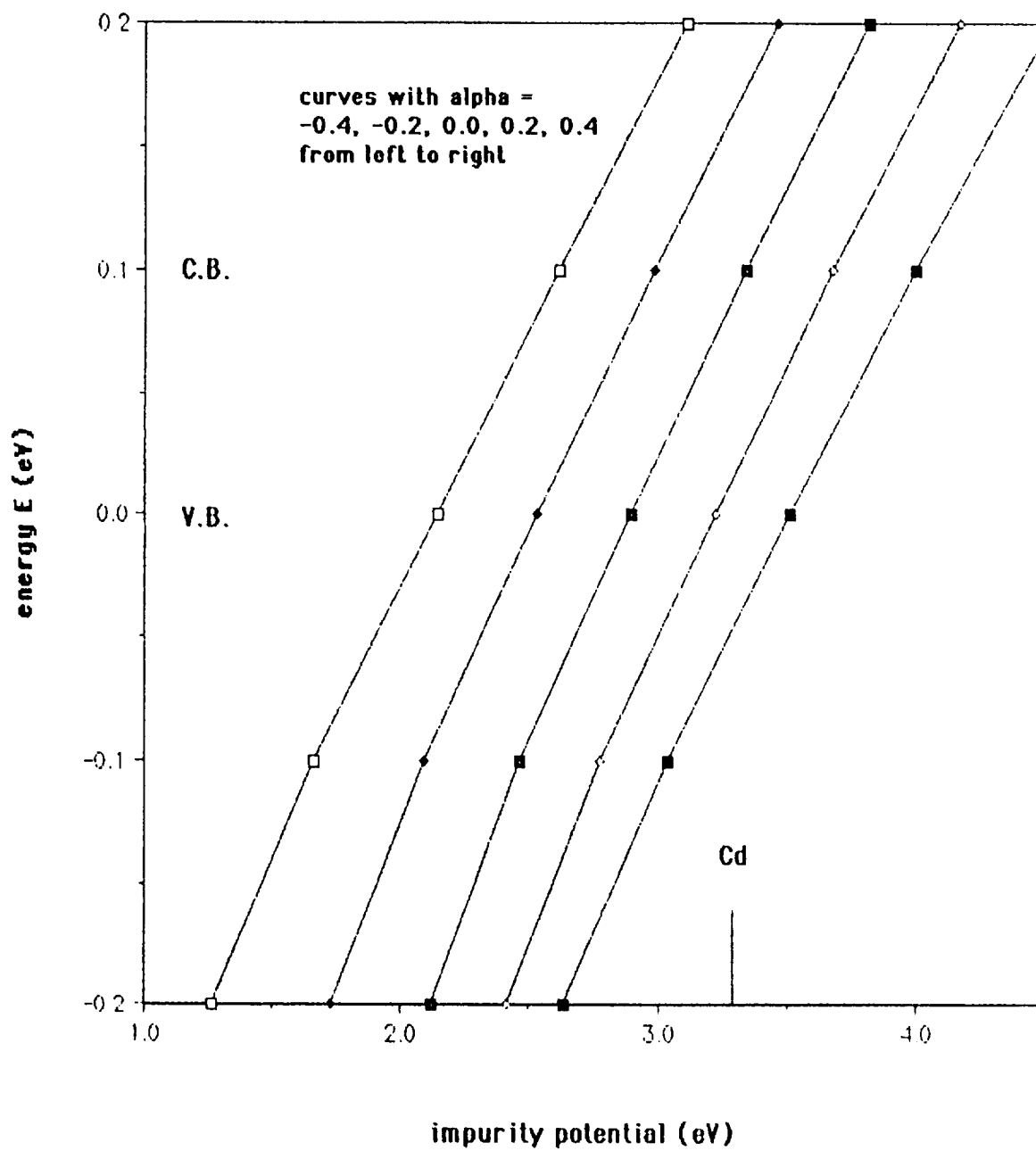


FIGURE 4

Effects of Lattice Relaxation on Deep Levels in MCT (anion site, p-like)

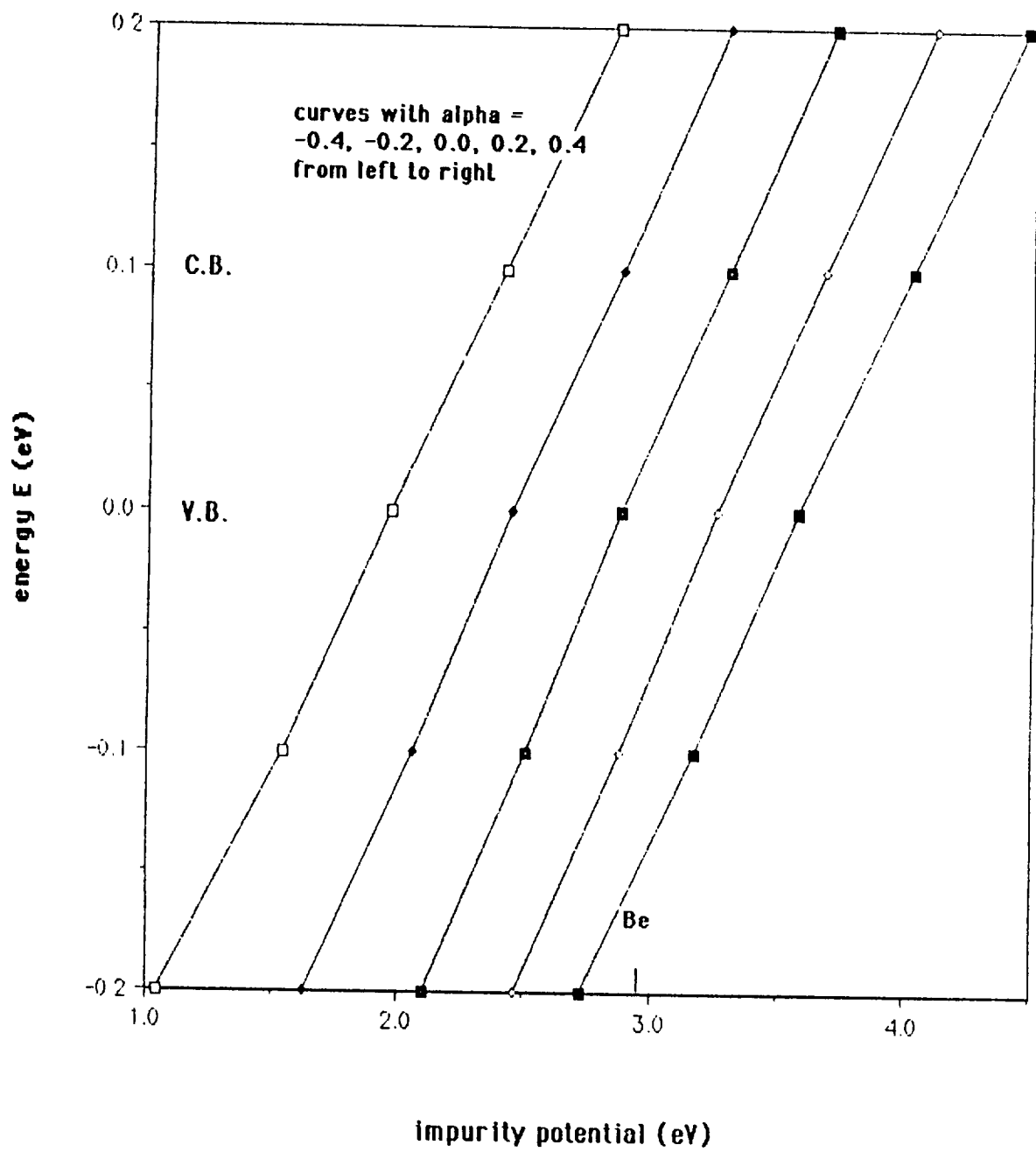


FIGURE 5

Effects of Lattice Relaxation on Deep Levels in MZS (anion site, p-like)

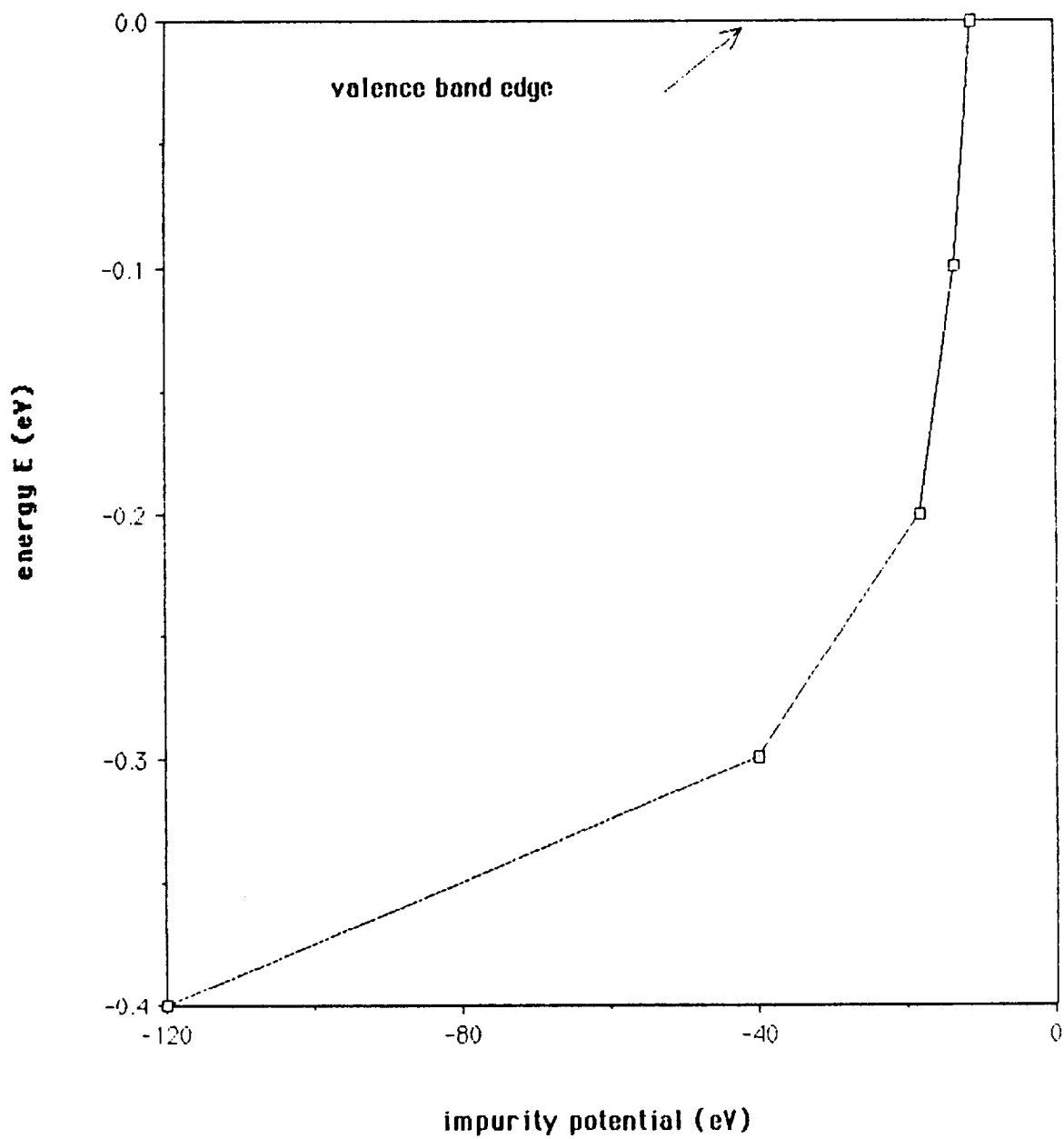


FIGURE 6

Vacancy Levels in MZT (cation site, p-like)

IV. APPENDICES

A. Some Basic References

1. S.T. Pantelides, "Deep Centers in Semiconductors," Gordon and Breach Science Publ. (1992).
2. S.T. Pantelides, "The Electronic Structure of Impurities and Other Point Defects in Semiconductors," *Rev. Modern Phys.* 50 797-858 (1978). Also, M. Lannoo and J. Bourgoin, "Point Defect in Semiconductors I: Theoretical Aspects," Springer-Verlag, Berlin (1981).
3. E.N. Economou, "Green's Functions in Quantum Physics," Springer-Verlag, Berlin (1990).
4. P. Vogl, H.P. Hjalmarson, and John D. Dow, "A Semi-Empirical Tight-Binding Theory of Electronic Structure of Semiconductors," *J. Phys. Chem. Solids* 44 (5), 365-378 (1983).
5. H.P. Hjalmarson, P. Vogl, D.J. Woford, and John D. Dow, "Theory of Substitutional Deep Traps in Covalent Semiconductors," *Phys. Rev. Letters* 44 (12), 810-813 (1980).
6. H.P. Hjalmarson, "Studies in the Theory of Solids," Ph.D. Thesis, The University of Illinois, 1979 (Unpublished).
7. S. Das Sarma and A. Madhukar, "Study of the ideal-vacancy-induced neutral deep levels in III-V compound semiconductors and their Ternary Alloys," *Phys. Rev. B* 24, 2051-2067 (1981).
8. Akiko Kobayashi, Otto F. Sankey, and John D. Dow, "Chemical Trends for Defect Energy Levels in $\text{Hg}_{1-x}\text{Cd}_x\text{Te}$," *Phys. Rev. B* 25, 6367-6379 (1982).
9. Wei-Gang Li and Charles W. Myles, "Effects of Lattice Relaxation on Deep Levels in Semiconductors," *Phys. Rev. B* 43, 2192-2200 (1991).
10. Wei-Gang Li and Charles W. Myles, "Molecular-Dynamics Approach to Lattice-Relaxation Effects on Deep Levels in Semiconductors," *Phys. Rev. B* 43, 9947-9950 (1991).
11. Wei-Gang Li and Charles W. Myles, "Deep-Level Wave Functions Including Lattice-Relaxation Effects," *Phys. Rev. B* 47, 4281-4288 (1993).

12. W.G. Li, "Effects of Lattice Relaxation on Deep Levels in Semiconductors," Ph.D. Thesis, Texas Tech University, 1991.
13. Walter A. Harrison, "Theory of the Two-Center Bond," Phys. Rev. B 27, 3592-3604 (1983).
14. S. Goettig and C.G. Morgan-Pond, "Formation Mechanism of Localized States in Tetrahedrally Bonded Semiconductors," Phys. Rev. B 42, 11743-11750 (1990).
15. E. Erbarut, "Electronic Structure of the Ideal Vacancies in (Hg Cd) Te," phys. stat. sol (b) 164, 235-241 (1991).
16. J.M. Luttinger and W. Kohn, "Motion of Electrons and Holes in Perturbed Periodic Fields," Phys. Rev. 97 869-883 (1954).
17. D.M. Larson, "Shallow Donor Levels of InSb in a Magnetic Field," J. Phys. Chem. Solids 29, 271-280 (1968).
18. E.O. Kane, "Band Structure of Indium Antimonide," J. Phys. Chem. Solids 1, 249-261 (1957).
19. G. Bastard, "Wave Mechanics Applied to Semiconductor Heterostructures," Halsted Press, 1988.
20. J.R. Lowney, A.H. Kahn, J.L. Blue, and C.L. Wilson, "Disappearance of impurity levels in silicon and germanium due to screening," J. applied Physics 52, 4075-4080 (1981).
21. M. Boukerche and J.P. Faurle, " The intrinsic and extrinsic doping of Mercury Cadmium Telluride grown by molecular beam epitaxy," in Shallow Impurities in Semiconductors 1988 (Edited by B. Monemar) Institute of Physics Conference Series No. 95, Bristol, 1989.

B. Green's Function⁽¹⁾

1. Summary of some standard Results⁽¹⁾

The results we list can be found, together with derivations, in the book by Economou.

The Green's function can be defined by

$$G(E) = \frac{1}{E - H} = \sum_n \frac{|n\rangle \langle n|}{E - E_n} \quad (\text{B1})$$

Define

$$G^\pm(\vec{r}, \vec{r}'; E) = \lim_{s \rightarrow 0^+} G(\vec{r}, \vec{r}'; E \pm is) \quad (\text{B2})$$

$$\text{where } G(\vec{r}, \vec{r}'; E) = \langle \vec{r} | G(E) | \vec{r}' \rangle \quad (\text{B3})$$

One can then show that the local density of states can be derived from

$$\rho(E) = \mp \frac{1}{\pi} \text{Im} \left[\text{Tr} (G^\pm(E)) \right] \quad (\text{B4})$$

where we have used:

$$\begin{aligned} G^\pm(\vec{r}, \vec{r}'; E) &= \lim_{s \rightarrow 0^+} \sum \frac{\phi_n(\vec{r}) \phi_n^*(\vec{r}')}{E \pm is - E_n} \\ &= P \sum_n \frac{\phi_n(\vec{r}) \phi_n^*(\vec{r}')}{E - E_n} \mp i \pi \sum_n \delta(E - E_n) \phi_n(\vec{r}) \phi_n^*(\vec{r}') \end{aligned} \quad (\text{B5})$$

Consider an unperturbed system with Hamiltonian H_0 and a perturbed system with Hamiltonian H_1 . Let the corresponding Green's function be G_0 and G where

$$\begin{aligned} G_0(z) &= (z - H_0)^{-1} \\ G(z) &= (z - H)^{-1} \end{aligned} \quad (\text{B6})$$

From this one can derive the Dyson equation

$$G = G_0 + G_0 H_1 G \quad (\text{B7})$$

And if one defines T matrix as

$$T = H_1 G G_0^{-1} \quad (\text{B8})$$

one can show

$$G(z) = G_0(z) + G_0 T G_0, \quad (\text{B9})$$

thus from the T matrix, we can determine the Green's function.

We now apply this to a crystal with an unperturbed tight binding Hamiltonian given by

$$H_0 = \epsilon_0 \sum_l |l\rangle \langle l| + \sum_m |l\rangle V_{\vec{l}m} \langle m| \quad (\text{B10})$$

where we will restrict $V_{\vec{l}m}$ to be \underline{V} for l and m being nearest neighbors and \underline{Q} otherwise.

Note $|l\rangle$ is the atomic-like orbital, or Wannier function, centered at lattice site \vec{l} .

We will consider only one band. The Bloch and Wannier functions are related by;

$$|\vec{k}\rangle = \frac{1}{\sqrt{N}} \sum_{\vec{l}} e^{i\vec{k}\cdot\vec{l}} |l\rangle \quad (\text{B11})$$

Since $H_0 |\vec{k}\rangle = E(\vec{k}) |\vec{k}\rangle$, we can show;

$$E(\vec{k}) = \epsilon_0 + \sum_{l(n.n)} e^{i\vec{k}\cdot\vec{l}} V_{\vec{l}}, \quad (\text{B12})$$

the typical tight binding result. Knowing the exact energy eigenvalues we can then evaluate the unperturbed Green's function.

To show how this is useful we consider a simple model of a substitutional impurity in a lattice as given by Economou. In Economou's model the substitutional impurity has as a perturbation

$$H_1 = |\vec{l}\rangle \varepsilon \langle \vec{l} | \quad (\text{B13})$$

From this, one can obtain the T matrix as

$$T = |\vec{l}\rangle \frac{\varepsilon}{1 - \varepsilon G_o(\vec{l}, \vec{l}; E)} \langle \vec{l} | \quad (\text{B14})$$

where $G_o(l, l; E) = \langle \vec{l} | G_o^{(E)} | \vec{l} \rangle$

The Green's function is then given by;

$$G = G_o + G_o |\vec{l}\rangle \frac{\varepsilon}{1 - \varepsilon G_o(l, l)} \langle \vec{l} | G_o \quad (\text{B15})$$

Then the poles of G yield the discrete eigenvalues (E_p) of H via

$$G_o(\vec{l}, \vec{l}, E_p) = 1/\varepsilon. \quad (\text{B16})$$

One might also mention that an ideal vacancy is modeled by assuming $\varepsilon \rightarrow \infty$ or

$$G_o(\vec{l}, \vec{l}, E_p) = 0 \quad (\text{B17})$$

which then excludes the site \vec{l} from occupancy.

2. Analytical Results

The Green function $G_o(E - H_o)^{-1}$ has a singularity at $E = E_{n\vec{k}}$, the eigenvalues of H_o . The singularity may be by-passed by including complex values

$$G_o^\pm(E) = \lim_{\varepsilon \rightarrow 0} \frac{L}{E - H_o \pm i\varepsilon} \quad (\text{B18})$$

But

$$\lim_{\varepsilon \rightarrow 0} \frac{L}{E \pm i\varepsilon} = P \frac{1}{E} \mp i\pi \delta(E) \quad (\text{B19})$$

where the principal value is defined by

$$P \int_a^b \frac{f(x)}{x - x_o} = \lim_{\delta \rightarrow 0} L \left[\int_a^{x_o - \delta} \frac{f(x) dx}{x - x_o} + \int_{x_o + \delta}^b \frac{f(x) dx}{x - x_o} \right] \quad (\text{B20})$$

Thus

$$G_o^\pm(E) = P \frac{1}{E - H_o} \mp \delta(E - H_o) (i\pi) \quad (\text{B21})$$

and the first term on the right hand side can be rewritten (formally)

$$G_o^\pm(E) = P \int \frac{\delta(E' - H_o)}{E - E'} dE' \mp (i\pi) \delta(E - H_o) \quad (\text{B22})$$

which is another form of (B5).

Away from the singularities we can write

$$G_o^\pm(E) = G_o(E) = \int \frac{\delta(E' - H^o)}{E - E'} dE' \quad (B23)$$

Using the identity

$$\delta(E' - H^o) = \sum_{nk} |nk\rangle \delta(E' - E_{nk}) \langle nk| \quad (B24)$$

$$G_o(E) = \sum_{nk} \int \frac{|nk\rangle \delta(E' - E_{nk}) \langle nk|}{E - E'} dE' \quad (B25)$$

Using $|l\rangle$ to denote Wannier state localized at site l .

$$\langle l | G_o(E) | l' \rangle = \sum_{nk} \int \frac{\langle l | nk \rangle \delta(E' - E_{nk}) \langle nk | l' \rangle}{E - E'} dE' \quad (B26)$$

$$\langle l | G_o(E) | l' \rangle = \sum_{nk} \frac{\langle l | nk \rangle \langle nk | l' \rangle}{E - E_{nk}} \quad (B27)$$

Finally, it is very useful for relaxation calculations to derive an expression for the force in neighboring ions.

Formally, the total energy can be written as

$$E_{tot} = \int_{-\infty}^{E_F} E \rho(E) dE \quad (B28)$$

where $\rho(E)$ is the density of states.

The force on one of the nearest-neighbor atoms can be represented as

$$F_x = -\frac{\partial E_{\text{tot}}}{\partial x} = -\frac{\partial}{\partial x} \int E \rho(E) dE \quad (\text{B29})$$

and x is along the defect-host bond direction. More precisely, this doesn't treat the core electrons which give repulsion, so this is only for the attractive electrons, F_x^a . A basic result is (Eq. B4)

$$\rho(E) = \mp \frac{1}{\pi} \text{Im} \left[\text{Tr} G_{(E)}^{\pm} \right] \quad (\text{B30})$$

Thus

$$F_x^a = + \frac{\partial}{\partial x} \int_{-\infty}^{E_F} E \frac{1}{\pi} \text{Im} \left[\text{Tr} G^+(E) \right] dE \quad (\text{B31})$$

Dyson's equation works for $G(z)$, so it certainly works for $G^+(E)$ which is just a limit of $G(z)$. Thus

$$G = G_o + G_o V G \quad (\text{B32})$$

or

$$\frac{\partial G}{\partial x} = G_o \frac{\partial V}{\partial x} G + G_o V \frac{\partial G}{\partial x} \quad \left(\frac{\partial G_o}{\partial x} = 0 \right) \quad (\text{B33})$$

so

$$(I - G_o V) \frac{\partial G}{\partial x} = G_o \frac{\partial V}{\partial x} G \quad (\text{B34})$$

which means

$$\frac{\partial G}{\partial x} = (I - G_o V)^{-1} G_o \frac{\partial V}{\partial x} G \quad (\text{B35})$$

From Dyson's equation it also follows that

$$G = (I - G_0 V)^{-1} G_0, \quad (\text{B36})$$

Thus we have

$$\frac{\partial G}{\partial x} = G \frac{\partial V}{\partial x} G \quad (\text{B37})$$

and

$$F_x^a = \frac{1}{\pi} \text{Im Tr} \int_{-\infty}^{E_F} E G \frac{\partial V}{\partial x} G dE \quad (\text{B38})$$

3. Determination of $G^0(E)$ - Vogl Band Structure Theory⁽²⁾

To calculate the defect levels from Eqn. (6), we need to calculate G_s^0 , G_p^0 first. In the Appendix B2, we have shown for E in the band gap as for defect levels (i.e. with $E \neq E_{nk}$), we have

$$G_o(E) = \int \frac{\delta(E' - H^0)}{E - E'} dE' \quad (B39)$$

We have also noted that the spectral density operator $\delta(E' - H^0)$ can be written as

$$\delta(E' - H^0) = \sum_{n\vec{k}} |n\vec{k}\rangle \delta(E - E_{n\vec{k}}) \langle n\vec{k}| \quad (B40)$$

Where $E_{n\vec{k}}$ and $|n\vec{k}\rangle$ are the eigenvalues and eigenvectors of the host crystal. In turn, $E_{n\vec{k}}$ and $|n\vec{k}\rangle$ can be determined from the model of H_o .

The model of H_o which has been used is based on the model of Vogl. The Hamiltonian of the perfect crystal has the form:

$$H_o = \sum \left(|i a \vec{R}\rangle E_j^a \langle i a \vec{R}| + |i c \vec{R}'\rangle E_j^c \langle i c \vec{R}'| \right) + \sum \left[|i a \vec{R}\rangle V_{ij} \langle j c \vec{R} + \vec{d}| + \text{h.c.} \right] \quad (B41)$$

where $i = s, p_x, p_y, p_z$ or s^* labels the orbitals, a and c denote anion (like Te^{2-}) or cation like ($\text{Hg}^{2+}, \text{Zn}^{2+}$), and h.c. denotes the Hermitian conjugate. The states $|i a \vec{R}\rangle$ and $|i c \vec{R}'\rangle$ are localized orbitals centered on the \vec{R} and the cation at $\vec{R} + \vec{d}$, respectively, where \vec{d} is the nearest neighbor distance.

The main points of this model as summarized by Vogl are

- (1) The chemistry of sp bonding is retained.
- (2) The diagonal matrix elements of the model are related to the atomic

energies of the chemical constituents. This is really what allows one to predict chemical trends.

- (3) The off-diagonal matrix elements scale as the inverse of the bond length.
- (4) The number of parameters in the model is minimal.
- (5) The theory reproduces both valence and conduction bands.

4. Determination of V - Hjalmarson's Deep Level Theory⁽³⁾

From Eqns. (6), (7) in section IIA, we see we need the perfect crystal Green's function G^0 and the defect potential V to determine the energy band. In the representation with symmetry appropriate to the symmetry of the point defect, V_s and V_p are matrices of a certain size, arising from Bloch diagonalization. With the five atom, central atom and nearest neighbors, cluster, V_s and V_p are 5×5 matrices. If we want to include the 2nd neighbor in the calculations, we need to consider a 17 atom cluster which includes a defect, 4 nearest neighbors, and 12 second neighbors so the matrices are 17×17 .

In Hjalmarson's deep level theory, four assumptions, described in detail in Hjalmarson's dissertation, are given. The assumptions are

- (1) Only consider the central cell potential (ignore the Coulomb potential). Thus this theory can only be used to predict the deep levels.
- (2) Use the nearest neighbor approximation so V_s and V_p are 5×5 matrices.
- (3) Assume the off-diagonal elements of V are equal to zero and thus ignore the effects of lattice relaxation.

Therefore, the form of V is diagonal and can be written:

$$V = \sum_i V_i = \sum_i |i a \vec{0}\rangle U_i \langle i a \vec{0}| \quad (\text{B42})$$

where the U_i are the diagonal elements of V_i and the basis states $|i a \vec{0}\rangle$ are orthogonalized symmetrized Lowdin orbitals which are linear combinations of sp^3 hybrid orbital. This assumption has been called the ideal defect assumption.

- (4) Assume the diagonal elements of the defect potential V_i can be calculated with the equations

$$U_s = \beta_s (E_{\text{imp}}^s - E_{\text{host}}^s) \quad (\text{B43})$$

$$U_p = \beta_p (E_{\text{imp}}^p - E_{\text{host}}^p) \quad (\text{B44})$$

where E_{imp} and E_{host} are the atomic orbital energies of defect and host atoms respectively, with β_s and β_p being proportional constants. Hjalmarson indicates that

$(E_{\text{imp}} - E_{\text{host}})$ changes by a constant factor on going from free ions to ions in a solid, so that this approximation puts in the correct chemical trends. Hjalmarson and others discuss empirical ways of fitting the β 's.

Because the V_s, V_p are diagonal, it is easy to show that the defect energies are determined by

$$U_s = 1/G_{aa}^s \quad \text{and} \quad U_p = 1/G_{aa}^p \quad (\text{B45})$$

Where G_{aa}^s and G_{aa}^p are the diagonal elements of the Green's function matrices G_s^o, G_p^o respectively.

C. Details of Shallow Impurity Levels⁽¹⁹⁾

Shallow Impurity Levels and the Kane Model

We start by reviewing the Kane $\vec{k} \cdot \vec{p}$ three band model. Kane diagonalized the Hamiltonian exactly for three bands (conduction, light hole, and split off). We write the basic Hamiltonian as

$$H = \frac{P^2}{2m_o} + V(r) \quad (C1)$$

where \vec{p} is the momentum operator, m_o is the electron mass and $V(r)$ is the crystal potential. Using Bloch's theorem

$$\psi_{\vec{k}}(\vec{r}) = \frac{1}{\sqrt{\Omega}} e^{i\vec{k} \cdot \vec{r}} U_{\vec{k}}(\vec{r}) \quad (C2)$$

where Ω is the volume of the crystal, \vec{k} is the Bloch wave vector and $U_{\vec{k}}(\vec{r})$ is periodic between unit cells. The time independent Schrodinger equation can then be written

$$\left[H_{k_o} + \frac{\hbar}{m_o} (\vec{k} - \vec{k}_o) \cdot \vec{p} + \frac{\hbar^2}{2m_o} (k^2 - k_o^2) \right] U_{nk}(\vec{r}) = E_n(\vec{k}) U_{nk}(\vec{r}) \quad (C3)$$

where

$$H_{k_o} = \frac{p^2}{2m_o} + V(\vec{r}) + \frac{\hbar}{m_o} \vec{k}_o \cdot \vec{p} + \frac{\hbar^2 k_o^2}{2m_o}. \quad (C4)$$

The band index is n .

The equations for the $\vec{k} \cdot \vec{p}$ representation are obtained by expanding the $U_{n\vec{k}}$ in terms of a set $U_{n\vec{k}_o}$.

$$U_{n\vec{k}}(\vec{r}) = \sum_{n'} K_{nn'} U_{n'\vec{k}_0}(\vec{r}) \quad (C5)$$

$$\rightarrow \text{If } \frac{1}{\Omega_0} \int_{\Omega_0} U_{n'\vec{k}}^*(\vec{r}) U_{n\vec{k}_0}(\vec{r}) d\mathbf{v} = \delta_{n'n} \quad (C6)$$

over a unit cell Ω_0 , then combining the last two equations, multiplying by $U_{n\vec{k}_0}^*$ and integrating over a unit cell, we find:

$$\sum_{n'} \left\{ \left[E_n(k_0) + \frac{\hbar^2}{2m_0} (k^2 - k_0^2) \right] \delta_{n'n} + \frac{\hbar}{m_0} (\vec{k} - \vec{k}_0) \cdot \vec{p}_{nn'} \right\} K_{nn'} = E_n(\vec{k}) K_{nn'} \quad (C7)$$

where

$$\vec{p}_{nn'} = \frac{1}{\Omega_0} \int_{\Omega_0} U_{n\vec{k}_0}^* \vec{p} U_{n'\vec{k}_0} d\mathbf{v}. \quad (C8)$$

The spin-orbit interaction must also be introduced. We ignore other relativistic interactions. This amounts to adding in

$$H_{so} = \frac{\hbar}{4m_0^2 C^2} (\vec{\sigma} \times \vec{\nabla} v) \cdot \vec{p} \quad (C9)$$

where $\vec{\sigma}$ is the Pauli operator.

Including the spin-orbit term one finds:

$$\begin{aligned}
& \sum_{n'} \left\{ [E_n(0) - E_n(\vec{k}) + \frac{\hbar^2 k^2}{2m_0}] \delta_{nn'} + \frac{\hbar}{m_0} \vec{k} \cdot \vec{p}_{nn'} \right. \\
& \quad + \frac{\hbar}{m_0} \frac{1}{4m_0 C^2} \langle n | (\vec{\sigma} \times \vec{\nabla} v) \cdot \vec{p} | n' \rangle \\
& \quad \left. + \frac{\hbar \vec{k}}{m_0} \cdot \frac{\hbar}{4m_0 C^2} \langle n | (\vec{\sigma} \times \vec{\nabla} v) | n' \rangle \right\} K_{nn'} = 0.
\end{aligned} \tag{C10}$$

Where the last term comes from going from $\psi_{n\vec{k}}$ to $U_{n\vec{k}}$ and is very small and will be neglected from here on out. We have chosen the Γ point where $k_0 = 0$ for Eqn (10).

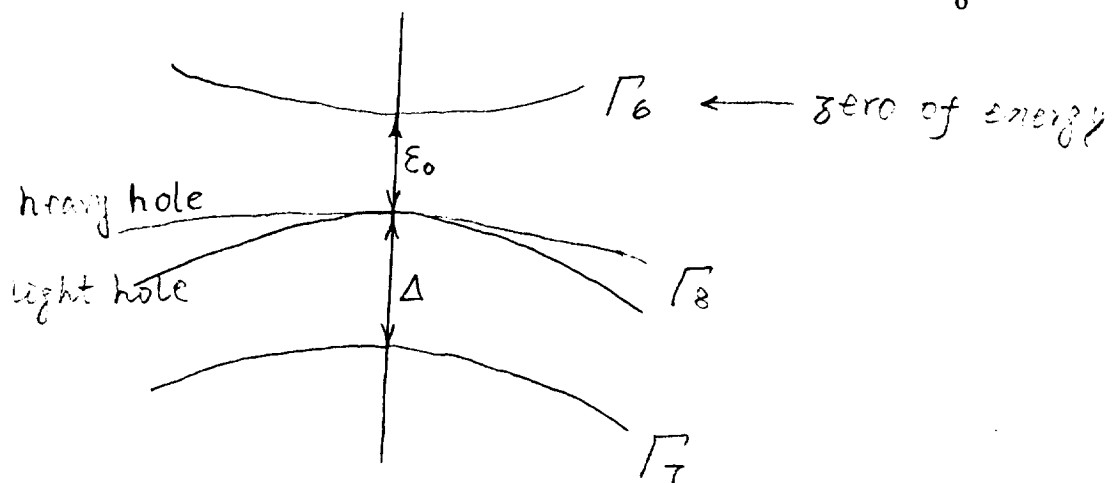
The approximation is often used that U_{n0} is restricted to states of $\Gamma_6, \Gamma_7,$ and Γ_8 symmetry - in the usual sense. These states include four bands (the conduction band, the light hole band, the split off band and the heavy hole band).

The basis functions for the bands, which diagonalize the spin-orbit interaction, will now be explained. We start with the functions $|s\rangle, |x\rangle, |y\rangle, |z\rangle$ which transform just like atomic s and p functions under the action of the tetrahedral group. Including spin, this gives 8 functions:

$|s\uparrow\rangle, |x\uparrow\rangle, |y\uparrow\rangle, |z\uparrow\rangle$ and $|s\downarrow\rangle, |x\downarrow\rangle, |y\downarrow\rangle$ and $|z\downarrow\rangle$. We then form linear combinations which diagonalize the spin orbit interaction.

In order to do this, we form linear combinations for which $\vec{J} = \vec{L} + \vec{S}$ and its projections J_z are diagonal. We summarize this in a table below, together with the band edge energies. This is a problem which is solved by Clebsch-Gordon coefficients. The U_n below are the periodic parts of the Bloch functions. In what follows we follow Bastard (1988) very closely, but add some details for clarity.

U_m	$J M_J$	Linear Combination	Energy of Band Edge (H=0)
$\frac{1}{2} \left(0 + \frac{1}{2} \right)$	$ \frac{1}{2}, \frac{1}{2}\rangle$	$i s\uparrow\rangle$	0
	$ \frac{1}{2}, -\frac{1}{2}\rangle$	$i s\downarrow\rangle$	0
$\frac{3}{4} \left(1 + \frac{1}{2} \right)$	$ \frac{3}{2}, \frac{1}{2}\rangle$	$-\sqrt{\frac{2}{3}} z\uparrow\rangle + \frac{1}{\sqrt{6}} (x+iy)\downarrow\rangle$	$-\epsilon_0$
	$ \frac{3}{2}, -\frac{1}{2}\rangle$	$-\sqrt{\frac{2}{3}} z\downarrow\rangle - \frac{1}{\sqrt{6}} (x-iy)\uparrow\rangle$	$-\epsilon_0$
	$ \frac{3}{2}, \frac{3}{2}\rangle$	$\frac{1}{\sqrt{2}} (x+iy)\uparrow\rangle$	$-\epsilon_0$
	$ \frac{3}{2}, -\frac{3}{2}\rangle$	$\frac{1}{\sqrt{2}} (1x-iy)\downarrow\rangle$	$-\epsilon_0$
$\frac{7}{8} \left(1 - \frac{1}{2} \right)$	$ \frac{1}{2}, \frac{1}{2}\rangle$	$\frac{1}{\sqrt{3}} (x+iy)\downarrow\rangle + \frac{1}{\sqrt{3}} z\uparrow\rangle$	$-\epsilon_0 - \Delta$
	$ \frac{1}{2}, -\frac{1}{2}\rangle$	$-\frac{1}{\sqrt{3}} (x-iy)\uparrow\rangle + \frac{1}{\sqrt{3}} z\downarrow\rangle$	$-\epsilon_0 - \Delta$



We will display the matrix of the Hamiltonian later, but for now we give some results. The secular equation for the energy is;

$$E^3 + (\Delta - E_g)E^2 - (E_g\Delta + P^2 k^2)E - \frac{2}{3}\Delta P^2 k^2 = 0, \quad (\text{C11})$$

from the three coupled bands. The heavy hole band decouples and comes out dispersionless. However, coupling of the heavy hole band to higher bands leads to

$$E_{hh} = \frac{\hbar^2 k^2}{2m_{hh}} \quad (\text{C12})$$

The momentum matrix element \underline{P} and the spin-orbit splitting parameter Δ are defined by

$$P = -\frac{i\hbar}{m_o} \langle s | P_x | x \rangle \quad (\text{C13a})$$

and

$$\Delta = -3i \left(\frac{\hbar}{4m_o^2 C^2} \right) \langle x | (\nabla \vec{V} \times \vec{P})_z | z \rangle. \quad (\text{C13b})$$

Our next job is to work out the matrix elements. We drop the k-dependent spin-orbit term as well as the relativistic corrections.

$$\begin{aligned} M_{ij} = & (E_i(o)) + \frac{\hbar^2 k^2}{2m_o} \delta_{ij} + \frac{\hbar}{m_o} \vec{k} \cdot \vec{P}_{ij} \\ & + \frac{\hbar}{m_o} \frac{1}{4m_o C^2} \langle i | (\vec{\sigma} \times \nabla V) \cdot \vec{P} | j \rangle \end{aligned} \quad (\text{C14})$$

The results are the following:

$$M = \begin{array}{c|cccccccc} & 1 & 2 & 3 & 4 & 5 & 6 & 7 & 8 \\ \hline 1 & \frac{\hbar^2 k^2}{2m_0} & 0 & -\frac{\sqrt{2}}{\sqrt{3}} P \hbar k_z & -\frac{1}{\sqrt{3}} P \hbar k_- & P \hbar k_+ & 0 & \frac{1}{\sqrt{3}} P \hbar k_z & -\frac{\sqrt{2}}{\sqrt{3}} P \hbar k_- \\ \hline 2 & 0 & \frac{\hbar^2 k^2}{2m_0} & \frac{P}{\sqrt{3}} \hbar k_+ & -\frac{\sqrt{2}}{\sqrt{3}} P \hbar k_z & 0 & P \hbar k_- & \frac{\sqrt{2}}{\sqrt{3}} P \hbar k_+ & \frac{1}{\sqrt{3}} P \hbar k_z \\ \hline 3 & -\frac{\sqrt{2}}{\sqrt{3}} P \hbar k_z & \frac{P}{\sqrt{3}} \hbar k_- & -\varepsilon_0 + \frac{\hbar^2 k^2}{2m_0} & 0 & 0 & 0 & 0 & 0 \\ \hline 4 & -\frac{1}{\sqrt{3}} P \hbar k_+ & -\frac{\sqrt{2}}{\sqrt{3}} P \hbar k_z & 0 & -\varepsilon_0 + \frac{\hbar^2 k^2}{2m_0} & 0 & 0 & 0 & 0 \\ \hline 5 & P \hbar k_- & 0 & 0 & 0 & -\varepsilon_0 + \frac{\hbar^2 k^2}{2m_0} & 0 & 0 & 0 \\ \hline 6 & 0 & P \hbar k_+ & 0 & 0 & 0 & -\varepsilon_0 + \frac{\hbar^2 k^2}{2m_0} & 0 & 0 \\ \hline 7 & \frac{1}{\sqrt{3}} P \hbar k_z & \frac{\sqrt{2}}{\sqrt{3}} P \hbar k_- & 0 & 0 & 0 & 0 & -\varepsilon_0 - \Delta + \frac{\hbar^2 k^2}{2m_0} & 0 \\ \hline 8 & -\frac{\sqrt{2}}{\sqrt{3}} P \hbar k_+ & \frac{P}{\sqrt{3}} \hbar k_z & 0 & 0 & 0 & 0 & 0 & -\varepsilon_0 - \Delta + \frac{\hbar^2 k^2}{2m_0} \end{array}$$

(C15)

Shallow Defects

We want to describe the behavior of electrons moving in imperfect III-V and II-VI crystals with defects. We look for solutions of the time independent Schrodinger equation

$$\left[H_0 + \phi(\vec{r}) \right] \psi(\vec{r}) = \epsilon \psi(\vec{r}) \quad (\text{C16})$$

where H_0 is the Hamiltonian of the perfect crystal and $\phi(\vec{r})$ is the non-periodic potential arising from the defect. For shallow defects, $\phi(\vec{r})$ is slowly varying at the scale of the unit cell.

We first prove some initial results. Consider the integral

$$I = \int_{\Omega} f(\vec{r}) p(\vec{r}) dV \quad (\text{C17})$$

where $p(\vec{r})$ has the periodicity of the lattice.

$$p(\vec{r} + \vec{R}) = p(\vec{r}) \quad (\text{C18})$$

$$\text{and } \vec{R} = \sum n_i \hat{e}_i \quad (\text{C19})$$

with n_i ($i = 1, 2, 3$) being integers and \hat{e}_i the fundamental translation vectors of the lattice. f is required to fall off quickly enough at large distances for I to converge and $p(\vec{r})$ is periodic. It can be expanded in a Fourier expansion using only the reciprocal lattice vector \vec{K} .

$$p(\vec{r}) = \sum_{\vec{K}} p(\vec{K}) e^{i\vec{K} \cdot \vec{r}} \quad (\text{C20})$$

where by inversion

$$\begin{aligned}
p(\vec{K}) &= \frac{1}{\Omega} \int_{\Omega} p(\vec{r}) e^{-i\vec{K} \cdot \vec{r}} d\mathbf{v} \\
&= \frac{1}{\Omega_0} \int_{\Omega_0} p(\vec{r}) e^{-i\vec{K} \cdot \vec{r}} d\mathbf{v},
\end{aligned} \tag{C21}$$

where Ω is the volume of the crystal and Ω_0 is the volume of the unit cell.

An approximate form for the integral below can be derived. This form of integral occurs later and we need to approximate it.

$$\begin{aligned}
I &= \int_{\Omega} f(\vec{r}) p(\vec{r}) d\mathbf{v} \\
&= \sum_{\vec{K}} p(\vec{K}) \int_{\Omega} f(\vec{r}) e^{i\vec{K} \cdot \vec{r}} d\mathbf{v}.
\end{aligned} \tag{C22}$$

Since the volume of the unit cell can be decomposed into identical stacked unit cells, we can write

$$\int_{\Omega} f(\vec{r}) e^{i\vec{K} \cdot \vec{r}} d\mathbf{v} = \sum_{\vec{R}_i} \int_{\Omega_i} f(\vec{R}_i + \vec{r}) e^{i\vec{K} \cdot \vec{r}} d\vec{r},$$

where we have used $e^{i\vec{K} \cdot \vec{R}} = 1$.

On the scale of a unit cell, we assume $f(\vec{r})$ is slowly varying so

$$f(\vec{R}_i + \vec{r}) \approx f(\vec{R}_i). \tag{C23}$$

Thus

$$\begin{aligned}
\int_{\Omega} f(\vec{r}) p(\vec{r}) d\mathbf{v} &\approx \sum_{\vec{R}_i} f(\vec{R}_i) \int_{\Omega_i} e^{i\vec{K} \cdot \vec{r}} d\mathbf{v} \\
&= \Omega_0 \delta_{\vec{K}}^0 \sum_{\vec{R}_i} f(\vec{R}_i).
\end{aligned} \tag{C24}$$

Thus

$$\begin{aligned}
 I &= \sum_{\vec{K}} P(\vec{K}) \Omega_o \delta_K^o \sum_{R_i} f(\vec{R}_i) \\
 &= p(o) \Omega_o \sum_{R_i} f(R_i) \\
 &= p(o) \int_{\Omega} f(\vec{r}) dv
 \end{aligned}$$

But $p(o) = \frac{1}{\Omega} \int_{\Omega} p(\vec{r}) dv$, so

we find

$$I \cong \frac{1}{\Omega} \left(\int_{\Omega} p(\vec{r}) dv \right) \left(\int_{\Omega} f(\vec{r}) dv \right). \quad (C25)$$

We have assumed the Bloch states $|n \vec{k}\rangle$ are normalized as per

$$\begin{aligned}
 \delta_{nn'} &= \frac{1}{\Omega} \int_{\Omega} U_{n\vec{k}}^*(\vec{r}) U_{n'\vec{k}} dv \quad (\text{whole crystal}) \\
 &= \frac{1}{\Omega_o} \int_{\Omega_o} U_{n\vec{k}}^*(\vec{r}) U_{n\vec{k}} dv \quad (\text{unit cell})
 \end{aligned} \quad (C26)$$

To solve $[H_o + \phi(\vec{r})] \psi(\vec{r}) = E \psi(\vec{r})$ (C27),

we assume $\phi(\vec{r})$ couples the $\Gamma_6, \Gamma_7, \Gamma_8$ states among themselves. Again, following a Kane like theory we look for a solution in the form

$$\psi(\vec{r}) = \sum_{l=1}^8 c_l f_l(\vec{r}) U_{l_o}(\vec{r}), \quad (C28)$$

where the $f_l(\vec{r})$'s are the envelope functions which vary slowly. The U_{l_o} 's are the

Γ point Bloch functions for the eight bands. When $\phi(\vec{r}) = 0$, we have $f_l = \frac{1}{\sqrt{\Omega}} e^{i\vec{k} \cdot \vec{r}}$

The wave function $\psi(\vec{r})$ is normalized so;

$$\begin{aligned}
1 &= \int_{\Omega} |\psi(\vec{r})|^2 d\mathbf{v} \\
&= \sum_{l,m} C_l C_m^* \int_{\Omega} f_m^* f_l U_{m_0}^* U_{l_0} d\mathbf{v}
\end{aligned}$$

Combining Eqs (17), and (25) for integrals of periodic and slowly varying functions, we have

$$1 = \sum_{l,m} C_l C_m^* \frac{1}{\Omega} \int f_m^* f_l d\mathbf{v} \int U_{m_0}^* U_{l_0} d\mathbf{v}$$

So we find ;

$$1 = \sum_l |c_l|^2 \int_{\Omega} |f_l|^2 d\mathbf{v} \tag{C29}$$

And again since we want $\sum |c_l|^2 = 1$, the envelope function needs to be normalized to 1.

Thus

$$\int_{\Omega} |f_l|^2 d\mathbf{v} = 1 \tag{C30}$$

In summary we have:

$$H_o = \frac{P^2}{2m_o} + v(\vec{r}) + \frac{\hbar}{4m_o^2 C^2} (\vec{\sigma} \times \vec{\nabla} V) \cdot \vec{P} \tag{C31}$$

$$\psi(\vec{r}) = \sum_{l=1}^8 C_l f_l(\vec{r}) U_{l_0}(\vec{r}) \tag{C32}$$

$$[H_o + \phi(\vec{r})] \psi(\vec{r}) = \epsilon \psi(\vec{r}) \tag{C33}$$

and f_l is normalized by Eq (30). We now substitute Eq (32) into (33) and use (31).

We use

$$p^2 (f_1 U_{1o}) = (p^2 f_1) U_1 + 2(p f_1)(p U_1) + f_1 (p^2 U_1). \quad (C34)$$

Let H_o be given by Eq (31), and as usual we will neglect the “k - dependent” part of the spin orbit interaction. We also set the notation so the spin orbit term is buried in H_o ,

$$H_o U_{1o} = \epsilon_{1o} U_{1o} \quad (C35)$$

So we get

$$\begin{aligned} 0 = & \sum_{l=1}^8 c_l ((\epsilon_{1o} - \epsilon)) \int f_m^* f_1 U_{1o} U_{mo}^* dv \\ & + \int_{\Omega} U_{mo}^* U_{1o} f_m^* \frac{p^2}{2m} f_1 dv \\ & + \frac{1}{m_o} \int_{\Omega} (U_{mo}^* \vec{p} U_{1o}) \cdot (f_m^* \vec{p} f_1) dv. \\ & + \int_{\Omega} f_m^* \phi(\vec{r}) f_1 U_{mo}^* U_{1o} dv \end{aligned} \quad (C36)$$

Using again Eq (25), we can simplify several integrals. We get

$$\begin{aligned} 0 = & \sum_{l=1}^8 c_l ((\epsilon_l - \epsilon)) \frac{1}{\Omega} \int f_m^* f_1 dv \int U_{mo}^* U_{1o} dv \\ & + \frac{1}{\Omega} \int f_m^* \frac{p^2}{2m_o} f_1 dv \int U_{mo}^* U_{1o} dv + \frac{1}{\Omega} \int f_m^* \phi(\vec{r}) f_1 \int U_{mo}^* U_{1o} dv \\ & + \vec{P}_{ml} \cdot \int f_m^* \vec{p} f_1 dv = 0, \end{aligned} \quad (C37)$$

where

$$\vec{P}_{ml} = \frac{1}{m_o} \frac{1}{\Omega} \int_{\Omega} U_{mo}^* \vec{p} U_{1o} dv, \quad (C38)$$

and we can use

$$\int U_{m_0}^* dv = \Omega \delta_m^1. \quad (\text{C39})$$

Therefore, we write

$$0 = \sum_{l=1}^8 C_l \{ (\epsilon_{l_0} - \epsilon) \int f_m^* f_l dv \delta_{lm} + \int f_m^* \frac{p^2}{2m_0} f_l dv \delta_{lm} + \int f_m^* \phi(\vec{r}) f_l dv \delta_{lm} + \vec{P}_{m1} \cdot \int f_m^* \vec{p} f_l dv \} \quad (\text{C40})$$

We can rewrite this as

$$0 = \int_{\Omega} dv f_m^*(\vec{r}) \sum_{l=1}^8 \left\{ \delta_{lm} \left[\epsilon_l - \epsilon + \frac{p^2}{2m_0} + \phi \right] + \vec{P}_{m1} \cdot \vec{P} \right\} C_l f_l,$$

where due to periodicity, we can rewrite Eq (38) as

$$\vec{P}_{m1} = \frac{1}{m_0 \Omega_0} \int U_{m_0}^* \vec{P} U_{1_0} dv. \quad (\text{C41})$$

Non vanishing solutions for f exist if f' is an eigensolution of the problem:

$$(D + \phi) \begin{pmatrix} f_1 \\ f_2 \\ \vdots \\ f_8 \end{pmatrix} = \epsilon \begin{pmatrix} f_1 \\ f_2 \\ \vdots \\ f_8 \end{pmatrix} \quad (\text{C42})$$

where $f_i' = C_i f_i$ and the matrix $D + \phi$ is given on the following page. We have dropped the free electron term and continue to neglect relativistic corrections and the 'k dependent' part of the spin orbit term.

The matrix for $D + \phi$ can be written:

	1	2	3	4	5	6	7	8
1	$\phi - \varepsilon$	0	$-\frac{\sqrt{2}}{\sqrt{3}} PP_z$	$-\frac{1}{\sqrt{3}} PP_-$	PP_+	0	$\frac{1}{\sqrt{3}} PP_z$	$-\frac{\sqrt{2}}{\sqrt{3}} PP_-$
2	0	$\phi - \varepsilon$	$\frac{1}{\sqrt{3}} PP_+$	$-\frac{\sqrt{2}}{\sqrt{3}} PP_z$	0	PP_-	$\frac{\sqrt{2}}{\sqrt{3}} PP_+$	$\frac{1}{\sqrt{3}} PP_z$
3	$-\frac{\sqrt{2}}{\sqrt{3}} PP_z$	$\frac{P}{\sqrt{3}} P_-$	$\phi - \varepsilon_0 - \varepsilon$	0	0	0	0	0
4	$-\frac{1}{\sqrt{3}} PP_+$	$-\frac{\sqrt{2}}{\sqrt{3}} PP_z$	0	$\phi - \varepsilon_0 - \varepsilon$	0	0	0	0
5	PP_-	0	0	0	$\phi - \varepsilon_0 - \varepsilon$	0	0	0
6	0	PP_+	0	0	0	$\phi - \varepsilon_0 - \varepsilon$	0	0
7	$\frac{1}{\sqrt{3}} PP_z$	$\frac{\sqrt{2}}{\sqrt{3}} PP_-$	0	0	0	0	$\phi - \Delta$ $-\varepsilon_0 - \varepsilon$	0
8	$-\frac{\sqrt{2}}{\sqrt{3}} PP_-$	$\frac{P}{\sqrt{3}} P_z$	0	0	0	0	0	$\phi - \Delta$ $-\varepsilon_0 - \varepsilon$

The periodic part of the Bloch functions going along with f_i are

$$\begin{aligned}
 & U_i \\
 & U_1 = i |s \uparrow \rangle \\
 & U_2 = i |s \downarrow \rangle \\
 & U_3 = -\sqrt{\frac{2}{3}} |z \uparrow \rangle + \frac{1}{\sqrt{6}} |(x+iy) \downarrow \rangle \\
 & U_4 = -\frac{1}{\sqrt{6}} |(x-iy) \uparrow \rangle - \sqrt{\frac{2}{3}} |z \downarrow \rangle \\
 & U_5 = \frac{1}{\sqrt{2}} |(x+iy) \uparrow \rangle \\
 & U_6 = \frac{1}{\sqrt{2}} |(x-iy) \downarrow \rangle \\
 & U_7 = \frac{1}{\sqrt{3}} |(x+iy) \downarrow \rangle + \frac{1}{\sqrt{3}} |z \uparrow \rangle \\
 & U_8 = -\frac{1}{\sqrt{3}} |(x-iy) \uparrow \rangle + \frac{1}{\sqrt{3}} |z \downarrow \rangle
 \end{aligned}$$

Eq (42) can be reduced to an effective 2 x 2 system starting with the third row, we get

$$-\sqrt{\frac{2}{3}} P P_z f_1 + \frac{P}{\sqrt{3}} P_- f_2 + (-\varepsilon - \varepsilon_0 + \phi) f_3 = 0,$$

or

$$f_3 = \frac{1}{(\varepsilon_0 + \varepsilon - \phi)} \left[-\sqrt{\frac{2}{3}} P P_z f_1 + \frac{P}{\sqrt{3}} P_- f_2 \right] \quad (\text{C43})$$

In a similar fashion, from the rest of the rows, we can derive:

$$f_4 = \frac{1}{(\varepsilon_0 + \varepsilon - \phi)} \left[-\frac{P}{\sqrt{3}} P_+ f_1 - \sqrt{\frac{2}{3}} P P_z f_2 \right] \quad (\text{C44})$$

$$f_5 = \frac{1}{(\varepsilon_0 + \varepsilon - \phi)} [P P_- f_1] \quad (\text{C45})$$

$$f_6 = \frac{1}{(\varepsilon_0 + \varepsilon - \phi)} [P P_+ f_2] \quad (\text{C46})$$

$$f_7 = \frac{1}{(\varepsilon_0 + \Delta + \varepsilon - \phi)} \left[\frac{P}{\sqrt{3}} P_z f_1 + P \sqrt{\frac{2}{3}} P_- f_2 \right] \quad (\text{C47})$$

$$f_8 = \frac{1}{(\varepsilon_0 + \Delta + \varepsilon - \phi)} \left[-\sqrt{\frac{2}{3}} P_+ f_1 + \frac{P}{\sqrt{3}} P_z f_2 \right] \quad (\text{C48})$$

If we substitute Eqs (43) - (48) into the two equations we get from the first two rows of Eq (42), we get our effective 2 x 2 Eq (42). This, in effect, projects the Eq into the Γ_6 band.

The resulting effective 2 x 2 equation can be written

$$\begin{bmatrix} H_d & H_{nd} \\ H_{nd}^+ & H_d \end{bmatrix} \begin{bmatrix} f_1 \\ f_2 \end{bmatrix} = \epsilon \begin{bmatrix} f_1 \\ f_2 \end{bmatrix} \quad (C49)$$

where

$$\begin{aligned} H_d = & \frac{2P^2}{3} p_z (\epsilon + \epsilon_o - \phi)^{-1} p_{z+} + P^2 p_{z+} (\epsilon + \epsilon_o - \phi)^{-1} p_- \\ & + \frac{P^2}{3} p_- (\epsilon + \epsilon_o - \phi)^{-1} p_+ + \frac{2P^2}{3} p_- (\epsilon + \epsilon_o + \Delta - \phi)^{-1} p_+ \\ & + \frac{P^2}{3} p_z (\epsilon + \epsilon_o + \Delta - \phi)^{-1} p_z + \phi \end{aligned} \quad (C50)$$

$$H_{nd} = \frac{\sqrt{2}}{3} P^2 \left[p_- \left\{ (\epsilon + \epsilon_o + \Delta - \phi)^{-1} - [\epsilon + \epsilon_o + \Delta - \phi]^{-1} \right\} p_z - p_z \left\{ [\epsilon + \epsilon_o - \phi]^{-1} - [\epsilon + \epsilon_o + \Delta - \phi]^{-1} \right\} p_- \right] \quad (C51)$$

Hydrogenic Donor Problem

$$\phi = e^2 / K r \quad (C52)$$

K = static dielectric constant of semiconductor.

For almost all r , $|\phi(\vec{r})| \ll \epsilon_o$

Expand to lowest order in

$$\frac{-\phi + \epsilon}{\epsilon_o} ; \quad \frac{-\phi + \epsilon}{\epsilon_o + \Delta}$$

We obtain
$$H_d^o = \frac{P^2}{2m_{\Gamma_6}} + \phi(\vec{r}) \quad (C53)$$

$$H_d = H_d^o - \frac{2P^2}{3\epsilon_o} \epsilon p^2 - \frac{P^2 \epsilon}{3(\epsilon_o + \Delta)^2} p^2 + \frac{2P^2}{3\epsilon_o} p_z \phi(\vec{r}) p_z$$

$$+ \frac{P^2}{2\epsilon_o} p_+ \phi(\vec{r}) p_+ + \frac{P^2}{3\epsilon_o} p_- \phi(\vec{r}) p_-$$

$$+ \frac{P^2}{3(\epsilon_o + \Delta)^2} p_z \phi(\vec{r}) p_z + \frac{2P^2}{3(\epsilon_o + \Delta)^2} p_- \phi(\vec{r}) p_+$$

$$H_{nd} = \frac{\sqrt{2}}{3} P^2 \left[\frac{1}{\epsilon_o} - \frac{1}{(\epsilon_o + \Delta)^2} \right] \left[p_- \phi(\vec{r}) p_z - p_z \phi(\vec{r}) p_- \right] \quad (C54)$$

With the zero order term only get Hydrogenic levels

$$a_o^* = 0.53 \text{ \AA} \times K \times \frac{m_o}{m_{\Gamma_6}}$$

$$R_o^* = 13.6 \text{ eV} \times \frac{m_{\Gamma_6}}{K^2 m_o} \quad (C55)$$